Full Text View

Volume 32, Issue 11 (November 2002)

Journal of Physical Oceanography
Article: pp. 3299–3309 | Abstract | PDF (833K)

Evidence of a Barrier Layer in the Sulu and Celebes Seas

Peter C. Chu

Naval Ocean Analysis and Prediction Laboratory, Department of Oceanography, Naval Postgraduate School, Monterey, California

Qinyu Liu and Yinglai Jia

Physical Oceanography Laboratory, Ocean–Atmosphere Interaction and Climate Laboratory, Ocean University of Qingdao, Qingdao, China

Chenwu Fan

Naval Ocean Analysis and Prediction Laboratory, Department of Oceanography, Naval Postgraduate School, Monterey, California

(Manuscript received September 13, 2001, in final form June 4, 2002)

DOI: 10.1175/1520-0485(2002)032<3299:EOABLI>2.0.CO;2

ABSTRACT

Variability in the surface isothermal and mixed layers of the Sulu and Celebes Seas is examined using the conductivity–temperature–depth data from the Navy's Master Oceanographic Observational Data Set (MOODS). Vertical gradient is calculated to determine isothermal layer depth with a criterion of 0.05°C m^{-1} for temperature profiles and mixed layer depth with a criterion of 0.015 kg m^{-4} for density profiles. When the isothermal layer depth is larger than the mixed layer depth, the barrier layer occurs. This study shows that the barrier layer occurs often in the Sulu and Celebes Seas. In the Sulu Sea, the barrier layer has seasonal variability with a minimum occurrence (38%) and a minimum thickness (3 m) in May and a maximum occurrence (94%) and a maximum thickness (36.5 m) in September. In the Celebes Sea, the barrier layer thickness changes from a maximum (49.7–62.0 m) in March–April to a minimum (9.6 m) in June. Possible mechanisms responsible for the barrier layer formation are discussed. In the Sulu Sea, the barrier layer may be formed by both rainfall and stratification; in the Celebes Sea, a rain-formed mechanism seems a major factor.

1. Introduction

Search Google Scholar for:
- Peter C. Chu
- Qinyu Liu
- Yinglai Jia
- Chenwu Fan

A vertically quasi-uniform layer of temperature (isothermal layer), salinity (isohaline layer), and density (mixed layer) is often observed in the upper ocean. Underneath it, there exists a layer with strong vertical gradient such as the thermocline (in temperature), halocline (in salinity), and pycnocline (in density). The isothermal layer depth (H_T) is not necessarily identical to the isohaline layer depth (H_S) or the mixed layer depth (H_D). There are areas of the World Ocean where H_T is deeper than H_S or H_D (Lindstrom et al. 1987; Lukas and Lindstrom 1991; Sprintall and Tomczak 1992; You 1995; Kara et al. 2000). The layer difference between halocline and thermocline is defined as the barrier layer (BL), which has strong salinity stratification and weak (or neutral) temperature stratification (Fig. 1). The barrier layer thickness (BLT) is originally defined by the difference between H_T and H_S. However, in recent studies BLT is often referred to as the difference between H_T and H_D (e.g., Kara et al. 2000).

Less turbulence in the BL than in the isohaline layer due to strong salinity stratification isolates the isohaline layer from cool thermocline water. This process affects the ocean heat budget (Swenson and Hansen 1999) and the heat exchange with the atmosphere. Studies on BL and related physical mechanisms have been devoted to the open ocean such as in the equatorial Pacific with BLT from 20 to 40 m (e.g., Lukas and Lindstrom 1991; You 1998) and the North Pacific with BLT larger than 50 m (Kara et al. 2000). However, little attention has been given to BL that occurs in regional seas. We use the conductivity–temperature–depth (CTD) data from the U.S. Navy's Master Oceanographic Observational Data Set (MOODS) for the Sulu and Celebes Seas to demonstrate the existence and variability of the BL in regional seas. The outline of this paper is as follows. A description of the Sulu/Celebes Seas is given in section 2. The MOODS–CTD data are depicted in section 3. Criteria for determining isothermal and mixed layers are discussed in section 4. A description of BL in the Sulu and Celebes Seas is given in sections 5 and 6. Physical processes for the BL formation are depicted in section 7. In section 8 we present the conclusions.

2. Sulu and Celebes Seas

The Sulu and Celebes Seas are the two major marginal seas in the outer southeastern Asia region (Fig. 2), which consists of an island arc stretching across near 5150 km along the equator at about 15°N–11°S and 94°–141°E, and which has two contrasting zones (Arief 1998). The Sulu Sea belongs to the western zone, where approximately 15%–20% of the global freshwater discharge enters (Toole 1987) through high annual rainfall, between 2 and 4 m yr^{-1} (ASEAN Subcommittee on Climatology 1982). The Celebes Sea belongs to the eastern zone, which is composed of deep-basin chains of depth 1000–4000 m and filled mainly by western Pacific water masses. This zone has annual rainfall less than 2 m yr^{-1} (ASEAN Subcommittee on Climatology 1982).

3. MOODS-CTD data

The temperature and salinity data for the Sulu Sea (8°–12°N, 117°–123°E) and the Celebes Sea (0°–6°N, 117°–126°E) acquired from MOODS went through quality control procedures such as a min–max check (e.g., disregarding any temperature data less than −2°C and greater than 35°C), error anomaly check (e.g., rejecting temperature data deviating more than 7°C from climatology), ship-tracking algorithm (screening out data with obvious ship position errors), max number limit (limiting a maximum number of observations within a specified and rarely exceeded space–time window), and buddy check (deleting contradicting data). The climatological data set used for the quality control is the U.S. Navy's Generalized Digital Environmental Model (GDEM) climatological temperature and salinity dataset. After quality control, there are 221 (278) CTD stations in the Sulu (Celebes) Sea. The majority of the CTDs were nominally capable of reaching a maximum depth of 2000 m.

The temporal and spatial distribution of MOODS–CTD data in the Sulu/Celebes Seas is irregular. Certain periods and areas are very well sampled while others lack enough observations to gain any meaningful insights. For example, there is a minimum (maximum) number of CTD stations in the Sulu Sea in May (July). There are no observations in the whole Sulu (Celebes) Sea in certain years (e.g., 1942–46, 1952–63 for the Sulu Sea, and 1979–88 for the Celebes Sea) and there are many observations in other years (e.g., 75 profiles in the Sulu Sea in 1949, and 52 profiles in the Celebes Sea in 1941). Spatial and temporal irregularities along with the lack of data in certain regions must be carefully weighted in order to avoid statistically induced variability.

4. Criteria for determining H_T and H_D

a. Existing criteria

There are two types of criteria, difference and gradient, for determining H_T and H_D in the upper ocean. The difference criterion requires the deviation of temperature (density) from its surface value to be smaller than a certain fixed value. The gradient criterion requires the vertical derivative of temperature (density) to be smaller than a certain fixed value.

1) DIFFERENCE CRITERIA

The criterion for determining H_T varies from 0.5°C (Wyrtki 1964; Monterey and Levitus 1997) to 0.8°C (Kara et al. 2000). The criterion for determining H_D is given by (Miller 1976; Spall 1991)

$$\Delta\sigma_t = 0.125\sigma_t(0), \quad (1)$$

or by (Sprintall and Tomczak 1992; Ohlmann et al. 1996; Monterey and Levitus 1997)

$$\Delta\sigma_t = 0.5°\text{C}(\partial\sigma_t/\partial T), \quad (2)$$

respectively. Here $\partial\sigma_t/\partial T$ is the thermal expansion coefficient evaluated using the surface values of temperature and salinity. The difference criterion (2) is based on the assumptions that the salinity effect on seawater expansion is negligible and that H_D is corresponding to the depth with temperature difference of 0.5°C from the surface (Sprintall and Tomczak 1992).

2) GRADIENT CRITERIA

Defant (1961) was among the first to use the gradient method. He uses a gradient of 0.015°C m^{-1} to determine H_T of the Atlantic Ocean. Bathen (1972) chose 0.02°C m^{-1}, and Lukas and Lindstrom (1991) used 0.025°C m^{-1}. The following gradient criterion is widely used (e.g., Lukas and Lindstrom 1991):

$$\partial\sigma_t/\partial z = 0.01 \text{ kg m}^{-4}. \quad (3)$$

b. Criteria used in this study

The gradient criteria

$$\partial T/\partial z = 0.05°\text{C m}^{-1}, \qquad \partial\sigma_t/\partial z = 0.01 \text{ kg m}^{-4} \quad (4)$$

are used here to determine H_T and H_D. This is because 1) the evident difference between the isothermal (isopycnal) layer and thermocline (pycnocline) is the vertical gradient, and 2) a recent observational study has shown that the mean H_T is less sensitive using gradient criteria than using difference criteria using 27 station data (You 1995). The mean H_T vary little among calculations based on

$$\partial T/\partial z = 0.05°\text{C m}^{-1}, \qquad \partial T/\partial z = 0.025°\text{C m}^{-1},$$
$$\partial T/\partial z = 0.015°\text{C m}^{-1}. \quad (5)$$

c. Threshold for determining BL

In the CTD measurements there are generally two thermometers, whose accuracy is about 0.02°C. Thus, the error in computing H_T is around 1 m using the gradient criterion (4). The density σ_t is computed from temperature and salinity. The error in computing H_D may be estimated by 2 m. Thus, the threshold for the BL is given as 3 m in this study.

5. Existence of BL in the Sulu Sea

a. General statistics

The two depths, H_T and H_D, are obtained from 221 CTD profiles using the gradient criteria (4). Monthly CTD stations

(denoted by the symbol "○") and the stations with the BL occurrence ($H_D < H_T$, represented by the symbol "+") in the Sulu Sea (Fig. 3) show a rather frequent occurrence of BL in the Sulu Sea. For example, among 16 (6) CTD stations in September (November), there are 15 (6) stations where a BL occurs. The rate of occurrence reaches 94% in September and 100% in November (Table 1). When BL occurs, the BLT is computed as the difference between H_T and H_D. The climatological characteristics are outlined as follows: (i) a BL occurs most frequently in September–November (fall) with a frequency of 90%–100% and least frequently in April and May (spring) with a frequency of 50%; (ii) The mixed layer depth (MLD) has a minimum value of 3 m in May and a maximum value of 30.5 m in February; and (iii) the BLT has large values in September–October (39.7–47.6 m) and small values of 9–11.3 m in April and May. It is noticed that the sample size is not sufficiently large; thus the statistical features mentioned here may have bias, especially in May.

b. Seasonal variability

Four groups of CTD data (Fig. 4) with relatively high sampling rates are selected to represent winter (January–February 1949, February–March 1972) and summer (July–September 1949, October 1973). Scatter diagrams of H_T and H_D (Fig. 5) show that the BL occurs quite often in both summer and winter and is more evident in the summer. For example, the MLD is much less than the isothermal depth (ITD) at almost all stations in October 1973. The maximum thickness of the BL (80 m) is found at Station 6 (see Fig. 4) with a MLD of 18 m and ITD of 98 m. Comparison among the four periods shows the BL has a relatively thin BLT in July–September 1949.

6. Existence of BL in the Celebes Sea

a. General statistics

The two depths (H_T and H_D) for the Celebes Sea are obtained from processing 179 CTD profiles using the gradient criteria (5). Monthly CTD stations (denoted by the symbol "○") and the stations with the BL occurrence ($H_D < H_T$, represented by the symbol "+") in the Celebes Sea (Fig. 6) show a rather frequent occurrence of BL in the Celebes Sea. For example, among 14 CTD stations in December, there are 13 stations where BL occurs. The rate of occurrence reaches 93% (Table 2). The BLT has a maximum value of 62.0 m in April and a minimum value of 9.6 m in June. The climatological features of a BL are outlined as follows: (i) the BL occurs most frequently in December with a frequency of 93% and least frequently in April with a frequency of 36%; (ii) the MLD has a minimum value of 7.3 m in March and a maximum value of 28.1 m in September; and (iii) the BLT has a maximum value in March–April (49.7–62.0 m) and a minimum value of 9.6 m in June. These numbers might not have statistical significance because of the small sample size.

b. Seasonal variability

Four groups of CTD data (Fig. 7) with relatively high sampling rates are selected to represent winter (January 1941), spring (May–June 1972), summer (July 1941), and fall (October 1978). Scatter diagrams of H_T and H_D (Fig. 8) show that the BL occurs quite often in winter and fall and less often in spring. For example, H_D is much less than H_T at almost all stations in January 1941. At Station 16, H_D and H_T are 25 and 100 m, respectively, with a BLT about 75 m. Among the four periods, the BL has relatively thin BLT in July 1941 and May–June 1972.

7. Discussion of physical processes causing the BL formation

a. Two mechanisms for the occurrence of BL

Two major factors determining H_T (H_D) are 1) surface winds and net heat (buoyancy) flux and 2) thermal (density) stratification underneath the isothermal (mixed) layer. Thus, the condition ($H_T > H_D$) is caused by the surface freshwater flux (precipitation excess over evaporation) and strong salinity stratification underneath the mixed layer. Thus, the BL can be classified as (i) rain formed, and (ii) stratification formed (weaker thermal and strong salinity stratification).

1) RAIN-FORMED MECHANISM

There are two regimes in the ocean mixed layer dynamics (e.g., Chu et al. 1990; Chu and Garwood 1991; Chu 1993): entrainment and detrainment. The detrainment process occurs with weak winds and strong surface warming (or excess precipitation over evaporation). The two depths H_T and H_D are determined by

$$H_T = \frac{C_1 u_*^3}{C_2 \alpha g F/\rho_0 c_p}, \qquad H_D = \frac{C_1 u_*^3}{C_2 B}, \qquad (6)$$

with C_1 and C_2 being tuning coefficients, g the gravity, α the thermal expansion coefficient, ρ_0 the characteristic density, c_p the specific heat under constant pressure, and F the net surface heat flux (downward positive). In a detrainment regime, $F > 0$. The ratio between the two depths is calculated by

$$\frac{H_T}{H_D} = 1 + \frac{\beta(P - E)S}{\alpha F/\rho_0 c_p}, \qquad (7)$$

where P and E are the precipitation and surface evaporation rate and β is the salinity contraction coefficient. Thus, the rain-formed mechanism ($P - E > 0$) becomes evident in the detrainment regime with weak winds, weak surface warming (low positive value of F), and strong surface freshwater flux [large positive value of $(P - E)$].

2) STRATIFICATION-FORMED MECHANISM

The stratification-formed mechanism is evident in the entrainment regime. Suppose that the rain-formed mechanism is absent ($P = E$) and that the initial H_T coincides with H_D:

$$H_T|_{t=0} = H_D|_{t=0}. \qquad (8)$$

The ratio of the initial entrainment velocities ($w_e = dH/dt$) between isothermal and mixed layers is given by (Chu 1993):

$$\frac{w_e^{(T)}}{w_e^{(D)}} = \frac{[-(\rho - \rho_{-H_D})]}{\alpha(T - T_{-H_T})}. \qquad (9)$$

A larger density jump

$$[-(\rho - \rho_{-H_D})] > \alpha(T - T_{-H_T}) \qquad (10)$$

leads to a larger entrainment velocity for the isothermal layer than for the mixed layer. Since the density stratification is determined by the temperature and salinity stratifications, the stratification-formed mechanism becomes important when the salinity stratification is strong. Thus, the stratification-formed mechanism becomes evident in the entrainment regime with strong winds, strong surface cooling (negative value of F), and strong salinity stratification. Usually, both rain-formed and stratification-formed mechanisms may take place at the same time, and precipitation may also strengthen the stratification.

b. Sulu Sea

The Comprehensive Ocean–Atmosphere Data Set (COADS) provides monthly mean sea surface wind stress and net heat and freshwater fluxes (Fig. 9). The surface wind stress, net heat flux (F), and net freshwater flux ($P - E$) have seasonal variability in the Sulu Sea. The wind stress strengthens in December–February [6.57–6.67 ($\times 10^{-2}$ N m^{-2})] and weakens in April–November [0.63–3.66 ($\times 10^{-2}$ N m^{-2})]. The net heat flux is negative in November–January (−25.4 to 0 W m^{-2}, surface cooling) and becomes large positive in March–May (60–110.3 W m^{-2}, strong surface warming). The surface freshwater flux ($P - E$) is weak in January–May (<0.6 m yr^{-1}) and strong in June–November (>1 m yr^{-1}).

In April and May the Sulu Sea is under the influence of weak winds [1.3–3 ($\times 10^{-2}$ N m^{-2})], strong net heat flux (60–110.3 W m^{-2}), and weak surface freshwater flux (0.52–0.56 m yr^{-1}). The strong heat flux and weak winds cause a shallow isothermal layer (small H_T). The weak freshwater flux cannot strengthen the salinity stratification. Thus, the BL occurs least frequently in April and May.

In September and October the Sulu Sea is under influence of weak winds [0.63–2.19 ($\times 10^{-2}$ N m^{-2})], weak net heat flux (24.6–29.2 W m^{-2}), and strong surface freshwater flux (3.1 m yr^{-1} in September). These conditions lead to the detrainment regime for the upper ocean and favor the rain-formed mechanism (excess precipitation over evaporation).

In December the Sulu Sea is under influence of strong winds (6.57 × 10^{-2} N m^{-2}), surface cooling (−25.4 W m^{-2}), and

relatively weak surface freshwater flux (0.8 m yr^{-1}). These conditions favor the entrainment regime in the upper ocean and the stratification-formed mechanism for the occurrence of a BL.

c. Celebes Sea

The surface wind stress, net heat flux (F), and net freshwater flux ($P - E$) have less seasonal variability in the Celebes Sea than in the Sulu Sea (Fig. 9). The wind stress varies between 0.45×10^{-2} (Nov) and 2.6×10^{-2} N m^{-2} (Feb). The surface net heat and freshwater fluxes are positive year-round with F varying from 17.5 (Jan) to 87.4 W m^{-2} (Mar) and ($P - E$) varying from 0.17 (Apr) to 2.1 m yr^{-1} (Jan). Thus, the Celebes Sea is under the influence of weak winds, surface warming, and surface freshwater flux all year. These conditions favor the rain-formed mechanism.

In December–January the Celebes Sea experiences weak net heat flux (17.5–24.5 W m^{-2}) and strong surface freshwater flux (1.14–2.06 m yr^{-1}). These conditions may cause the detrainment regime for the upper ocean and favor the rain-formed mechanism (excess precipitation over evaporation).

In April, the Celebes Sea experiences strong net heat flux (80.4 W m^{-2}) and weak surface freshwater flux (0.17 m yr^{-1}). The strong heat flux and weak winds cause a shallow isothermal layer (small H_T). The weak freshwater flux strengthens the salinity stratification slightly. Thus, the BL occurs least frequently in April.

8. Summary

1. Atmospheric forcing (rain-formed mechanism) and ocean physical processes (stratification-formed mechanism) may cause the occurrence of a barrier layer (deeper thermocline than pycnocline) in the Sulu/Celebes Seas. Using the U.S. Navy's Master Oceanographic Observational Data Set, we have shown barrier layer thickness up to 47.6 m (62.0 m) in the Sulu (Celebes) Sea.

2. The barrier layer appears quite often in both Sulu and Celebes Seas. The estimated occurrence rate varies from 50% (April and May) to 100% (November) in the Sulu Sea and from 36% (April) to 93% (December) in the Celebes Sea.

3. In the Sulu Sea, the mixed layer depth has a minimum value of 3 m in May and a maximum value of 30.5 m in February. The barrier layer thickness has large values in September–November (39.7–47.6 m) and small values of 9–11.3 m in April and May.

4. In the Celebes Sea, the mixed layer depth has a minimum value of 7.3 m in March and a maximum value of 28.1 m in September. The barrier layer thickness has large values in March–April (49.7–62.0 m) and small value of 9.6 m in June. Relatively higher precipitation and lower wind stress than for the Sulu Sea are found in winter (see Fig. 9).

5. In the Sulu Sea, both rain-formed and stratification-formed mechanisms are responsible for the barrier layer formation. However, in the Celebes Sea the rain-formed mechanism is responsible for the barrier layer formation.

Acknowledgments

This work was funded by the Naval Oceanographic Office, the Office of Naval Research, and the Naval Postgraduate School. Liu was also funded by the Chinese National Key Program for Developing Basic Science (G1999043807) and Chinese Special Program “2001DIA50041” of the National Ministry of Science and Technology.

REFERENCES

Arief D., 1998: Outer Southeast Asia: A region of deep straits, including the Benda Sea coastal segment (13°S). *The Sea,* A. R. Robinson and K. H. Brink, Eds., Regional Studies and Syntheses, Vol. 11, John Wiley and Sons, 507–522.

ASEAN Subcommittee on Climatology,, 1982: *The ASEAN Climatic Atlas*. Directorate of National Mapping, Kuala Lumpur, Malaysia, 104 pp.

Bathen K. H., 1972: On the seasonal changes in the depth of the mixed layer in the North Pacific Ocean. *J. Geophys. Res.*, **77**, 7138–7150. Find this article online

Chu P. C., 1993: Generation of low frequency unstable modes in a coupled equatorial troposphere and ocean mixed layer. *J. Atmos. Sci.*, **50**, 731–749. Find this article online

Chu P. C., and R. W. Garwood Jr.,, 1991: On the two-phase thermodynamics of the coupled cloud-ocean mixed layer. *J. Geophys. Res.*, **96**, 3425–3436. Find this article online

Chu P. C., R. W. Garwood Jr.,, and P. Muller, 1990: Unstable and damped modes in coupled ocean mixed layer and cloud models. *J. Mar. Syst.*, **1**, 1–11. Find this article online

Defant A., 1961: *Physical Oceanography*. Vol. 1. Pergamon, 729 pp.

Kara A. B., P. A. Rochford, and H. E. Hurlburt, 2000: Mixed layer depth variability and barrier layer formation over the North Pacific Ocean. *J. Geophys. Res.*, **105**, 16783–16801. Find this article online

Lindstrom E., R. Lukas, R. Fine, E. Firing, S. Godfrey, G. Meyers, and M. Tsuchiya, 1987: The Western Equatorial Pacific Ocean Circulation Study. *Nature*, **330**, 533–537. Find this article online

Lukas R., and E. Lindstrom, 1991: The mixed layer of the western equatorial Pacific Ocean. *J. Geophys. Res.*, **96**, 3343–3357. Find this article online

Miller J. R., 1976: The salinity effect in a mixed layer ocean model. *J. Phys. Oceanogr.*, **6**, 29–35. Find this article online

Monterey G., and S. Levitus, 1997: *Seasonal Variability of Mixed Layer Depth for the World Ocean*. NOAA Atlas NESDIS 14, 100 pp.

Ohlmann J. C., D. A. Siegel, and C. Gautier, 1996: Ocean mixed layer radiant heating and solar penetration: A global analysis. *J. Climate*, **9**, 2265–2280. Find this article online

Spall M. A., 1991: A diagnostic study of wind- and buoyancy-driven North Atlantic circulation. *J. Geophys. Res.*, **96**, 18509–18518. Find this article online

Sprintall J., and M. Tomczak, 1992: Evidence of barrier layer in the surface layer of tropics. *J. Geophys. Res.*, **97**, 7305–7316. Find this article online

Swenson M. S., and D. V. Hansen, 1999: Tropical Pacific Ocean mixed layer budget: The Pacific cold tongue. *J. Phys. Oceanogr.*, **29**, 69–81. Find this article online

Toole J. M., 1987: WOCE, interbasin exchanges, and marginal sea overflows. *Eos, Trans. Amer. Geophys. Union*, **68**(1), 211–3. Find this article online

Wyrtki K., 1964: The thermal structure of the eastern Pacific Ocean. *Dstch. Hydrogr. Z.*, **8A**, 6–84, (Suppl.),. Find this article online

You Y., 1995: Salinity variability and its role in the barrier-layer formation during TOGA–COARE. *J. Phys. Oceanogr.*, **25**, 2778–2807. Find this article online

You Y., 1998: Rain-formed barrier layer of the western equatorial Pacific warm pool: A case study. *J. Geophys. Res.*, **103**, 5361–5378. Find this article online

Tables

Table 1. Monthly occurrence frequency and climate features of the barrier layer in the Sulu Sea

Month	Jan	Feb	Mar	Apr	May	Jun	Jul	Aug	Sep	Oct	Nov	Dec	Total
N	12	13	19	8	2	61	16	19	16	31	6	18	221
B	8	11	17	4	1	48	11	16	15	28	6	14	179
B/*N* (%)	67	85	89	50	50	79	69	84	94	90	100	78	
Mean MLD (m)	29	30.5	19.5	16.5	3	16.4	14.2	12.9	11.1	14.9	21.2	12.1	
Mean BLT (m)	27.5	29.9	14.1	11.3	9.0	12.2	26.7	29.3	39.7	47.6	33.7	45.3	

Click on thumbnail for full-sized image.

Table 2. Monthly occurrence frequency and climate features of the barrier layer in the Celebes Sea

Month	Jan	Feb	Mar	Apr	May	Jun	Jul	Aug	Sep	Oct	Nov	Dec	Total
N	22	10	10	22	0	13	77	50	9	21	30	14	278
B	19	9	7	8	0	9	68	41	7	17	26	13	224
B/*N* (%)	86	90	70	36		69	88	82	78	81	87	93	
Mean MLD (m)	21.2	12.3	7.3	13.0		14.4	15.3	24.3	28.1	16.1	15.8	16.2	
Mean BLT (m)	41.1	26	49.7	62.0		9.6	27.9	30	11.3	20.7	15.3	16.8	

Click on thumbnail for full-sized image.

Figures

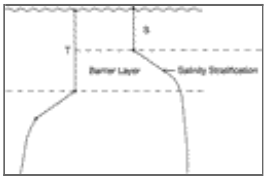

Click on thumbnail for full-sized image.

FIG. 1. A diagram of isothermal, mixed, and barrier layers

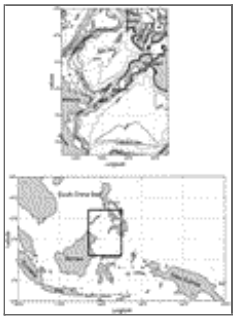

Click on thumbnail for full-sized image.

FIG. 2. Geographic and topographic presentation of the Sulu and Celebes Seas

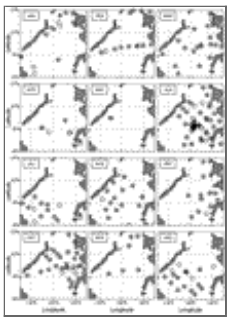

Click on thumbnail for full-sized image.

FIG. 3. Monthly CTD stations (denoted by "○") and the stations with BL occurrence ($H_D < H_T$; denoted by "+") in the Sulu Sea

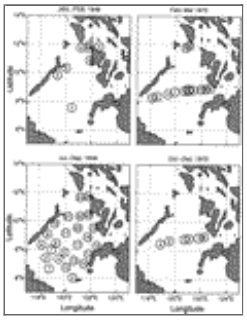

Click on thumbnail for full-sized image.

FIG. 4. CTD stations in the Sulu Sea for the four selected periods: (a) Jan–Feb 1949, (b) Feb–Mar 1972, (c) Jul–Sep 1949, and (d) Oct–Dec 1973

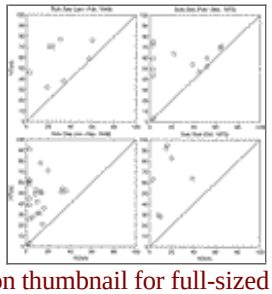

Click on thumbnail for full-sized image.

FIG. 5. Scatter diagrams (H_T vs H_D) of the Sulu Sea for the four selected periods: (a) Jan–Feb 1949, (b) Feb–Mar 1972, (c) Jul–Sep 1949, and (d) Oct–Dec 1973

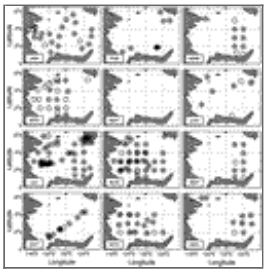

Click on thumbnail for full-sized image.

FIG. 6. Monthly CTD stations (denoted by "○") and the stations with BL occurrence ($H_D < H_T$; denoted by "+") in the Celebes Sea

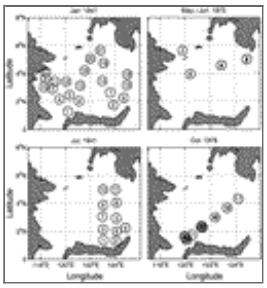

Click on thumbnail for full-sized image.

FIG. 7. CTD stations in the Celebes Sea for the four selected periods: (a) Jan–Feb 1949, (b) Feb–Mar 1972, (c) Jul–Sep 1949, and (d) Oct–Dec 1973

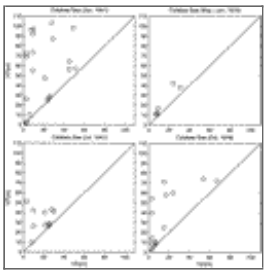

Click on thumbnail for full-sized image.

FIG. 8. Scatter diagrams (H_T vs H_D) of the Celebes Sea for the four selected periods: (a) Jan–Feb 1949, (b) Feb–Mar 1972, (c) Jul–Sep 1949, and (d) Oct–Dec 1973

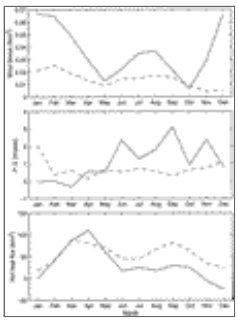

Click on thumbnail for full-sized image.

FIG. 9. Monthly mean COADS (a) surface wind stress (N m^{-2}), (b) $P - E$ (m yr^{-1}), and (c) net heat flux (W m^{-2}) averaged over the Sulu Sea (solid curve) and the Celebes Sea (dashed curve)

Corresponding author address: Dr. Peter C. Chu, Department of Oceanography, Naval Postgraduate School, Monterey, CA 93943-5100. E-mail: chu@nps.navy.mil

top